2020

Using Unmanned Aircraft Systems to Identify Invasive Species

Tithe Ahmed
Western Kentucky University, tithe.ahmed752@topper.wku.edu

USING UNMANNED AIRCRAFT SYSTEMS TO IDENTIFY INVASIVE SPECIES

A Capstone Experience/Thesis Project Presented in Partial Fulfillment
of the Requirements for the Degree Bachelor of Science
with Mahurin Honors College Graduate Distinction
at Western Kentucky University

By

Tithe Ahmed

May 2020

*****

CE/T Committee:

Dr. Michael Stokes, Advisor

Dr. Philip Lienesch

Prof. Joel Lenoir

ABSTRACT

Invasive species serve as a threat to native biodiversity and ecosystem sustainability. Combatting the spread of invasive species requires long-term physical and monetary commitments. In Balule Nature Reserve of Greater Kruger National Park, South Africa, *Opuntia ficus-inidica* (the common prickly pear) has been a relentless invader, displacing the local flora and fauna. The goal of this project is to battle invasive species such as prickly pear using efficient and inexpensive technology: unmanned aerial vehicles (UAVs or drones) and multispectral sensors.

Using a 4-bandwidth Parrot Sequoia multispectral sensor in tandem with the DJI Phantom Pro 3™ UAV, images of land plots were collected in the summer of 2018 on Balule Nature Reserve and surrounding areas in South Africa. From the images collected, maps were created using the mapping software Pix4D Mapper. Vegetation indices were created in which certain properties of vegetation are highlighted, assisting in plant identification. Using geographical informational system (GIS) software, classifications will be performed in which the multispectral data serves an important role. Multispectral sensors capture images in varying bandwidths; by collecting images in the red, green, red edge, and near-infrared bandwidths, there is potential for creating unique spectral signatures specific to individual objects such as prickly pear. Once a spectral signature is determined, a computer can then potentially perform unsupervised classifications to identify prickly pear solely from aerial images.

I dedicate this thesis to my friends, who supported me every step of the way.

I also dedicate this to my family, without whom I would not have had the courage to travel to South Africa. You inspire me every day to be better than I was the last. Lastly, I dedicate this work to anyone who funds themselves in bouts of self-doubt—you can do it.

ACKNOWLEDGEMENTS

This capstone project would not have been possible without the passion and intelligence of Dr. Michael Stokes, who pushed me every day to do and be better. It was a privilege of mine to have been mentored by you, and I hope to make you proud every day. We would like to thank all the personnel and volunteers at Balule Nature Reserve and Transfrontier Africa, including Craig Spencer, Paul Allin, and Chris Farren, for their dedication to science, conservation, and making the world a better place. This research would not have been possible without the gracious funding from the WKU Mahurin Honors College, FUSE Program, and the Gatton Academy of Mathematics and Science.

VITA

EDUCATION

Western Kentucky University, Bowling Green, KY B.S. in Biology – Mahurin Honors College Graduate Honors Capstone: *Using Unmanned Aircraft Systems to Detect Invasive Species*	May 2020
Gatton Academy of Mathematics and Science, Bowling Green, KY	May 2017
Glasgow High School, Glasgow, KY	May 2017

PROFESSIONAL EXPERIENCE

All Creatures Animal Hospital Student Worker	May. 2019- Present
Gatton Academy of Mathematics and Science, WKU Desk Assistant	Jan. 2019- May 2019

AWARDS & HONORS

Ernest O. Beal Biology Scholarship, WKU, June 2019
iFUSE Award, WKU, December 2018
World Topper Scholarship, WKU, March2018
Honors with Disctinction, Gatton Academy, May 2017

INTERNATIONAL EXPERIENCE

Study Abroad to South Africa, Hoedspruit, South Africa Graduate Biology 485: Field Biology African Wildlife Management & Research	May 2018- July 2018
Study Abroad to Costa Rica, Costa Rica Honors Biology 285: Costa Rican Biodiversity	Jan. 2017- Jan. 2017
Study Abroad to Harlaxton, Harlaxton, England English 200: Introduction to Literature	July 2016- Aug. 2016

CONTENTS

LIST OF FIGURES

LIST OF TABLES

INTRODUCTION

In the United States, it is estimated that approximately $120 billion are spent in damages due to invasive species every year (USFWS, 2012). These costs include, but are not limited to, prevention, detection, response, management, and habitat restoration (USFWS, 2012). Invasive species serve as a threat to native biodiversity and ecosystem sustainability (Lemke *et al.*, 2013). Often introduced to ecosystems by accident or for personal use, invasive plant species proliferate in the ecosystem to which they have been introduced by taking advantage of nutrients that would otherwise sustain the native vegetation. This creates a competition between invasive and native plants and deteriorates the ecosystem.

In South Africa, many invasive species have been introduced to provide food, raw materials, ecosystem control, or often by accident (Zengeya *et al.*, 2017). Some invasive plants that have spread across regions of South Africa and negatively affected the ecosystems they invaded are *Chromolaena odorata* (triffid weed), *Jacaranda mimosifolia* (jacaranda), and *Atriplex* species (saltbushes) (Richardson & Van Wilgen, 2004). These species displayed rapid growth in both size and range before biological agents were used to decrease their expansion. Many species of cacti, grasses, and tree species like acacias, eucalyptus and pines (Zengeya *et al.*, 2017) have also invaded the Eastern Cape, Gauteng, Free State, Mpumalanga, Limpopo, and the Western Cape provinces. One genus of cactus, *Opuntia,* is a significant invader of the Mpumalanga and Limpopo provinces (Invasive Species South Africa, 2019), wreaking havoc in Kruger National

Park and private nature reserves. Some species of *Opuntia* that have invaded South Africa are *O. aurantiaca* (jointed cactus), *O. ficus-indica* (the common prickly pear), and *O. humifusa* (eastern prickly pear) (Zengeya, 2017). *Opuntia* cacti are characterized by prickly cactus pads; many species also bear a spiny, pear-like fruit on top of the stalks. For this reason, *Opuntia* are nicknamed "prickly pear".

Figure 1- An image of Opuntia ficus-indica *(Rignanese, L. 2005)*

To combat the spread of prickly pear through the South African savanna, wildlife biologists and park personnel often must traverse the land by foot and search for individual prickly pear plants. Prickly pears and other invasive species can be eliminated through herbicides or biological control agents, such as insects or fungi like *Verticillium lecanii* and *Hirsutella thompsonii* (CABI, 2019) (Hall & Papierok, 1982). However, this method of searching for and eliminating prickly pear by foot is time-costly, expensive, dangerous due to the environment, and requires a lot of manual labor. Prickly pears are often also surrounded by tall grasses and thorny bushes and trees, making them hard to

reach or spot. To avoid these obstacles, scientists have begun exploring various methods of invasive species monitoring and habitat analysis.

Remote sensing is often utilized to detect, map and monitor wild vegetation, providing a plethora of methods to collect multispectral data and perform cost-effective habitat analysis (Joshi, *et al.*, 2004). Remote sensing can be achieved through satellite imagery or other multispectral or hyperspectral imagery, and it is often integrated with geographical information systems (GIS) to map plant distributions and invasive species patterns, creating decision support systems (Hegazy & Kaloop, 2015). Unmanned aerial vehicles (UAVs), when used with multispectral sensors, provide a means of capturing landscape images and vegetation structures at higher resolutions than satellite imagery and are more economical than using manned aircraft to survey ecosystems (Matese *et al.*, 2015; Carl *et al*., 2017). Multispectral sensors capture reflected electromagnetic energy in multiple, discrete-wavelength bands which provide information concerning land properties (Neha *et al.*, 2016). These data can be used to develop various vegetation indices to analyze land cover, providing detailed information about species distribution, soil properties, and condition of land.

Vegetation indices allow for precision agriculture, combining data from several spectral bands to accentuate vegetation properties such as canopy characteristics, radiation absorption, and chlorophyll content (Candiago, *et al*. 2015). Some commonly used vegetation indices include the Normalized Difference Vegetation Index (NDVI), Leaf Area Index (LAI), and Soil-Adjusted Vegetation Index (SAVI). In order to generate a vegetation index, remote images must first be obtained from sensors on a platform. Before modern technological advances in UAVs, these platforms were primarily satellites

and manned aircrafts (Candiago, et al., 2015). However, the images derived from these platforms were often of poor resolution. Using modern technology, more platforms are available readily and at low-cost, such as UAVs. Multispectral sensors on UAVs can capture images at a much higher resolution and provide more data in a shorter amount of time than can most satellite-acquired images

Images captured at different wavelengths on the electromagnetic spectrum highlight unique features within the spectral signature of an object (Turner, *et al*. 2003). For example, because the near-infrared band reflects light between 800 and 2500 nm on the electromagnetic spectrum, it can highlight moisture within plants, allowing for a statistical evaluation of vegetation moisture levels (Turner *et al.*, 2003). To make quantitative measurements, various aspects of energy, sensitivity, and absorption are combined. Because *Opuntia* are cacti, we considered moisture level an important aspect for potential identification using remotely sensed data. Other succulent plant species might be confused with *Opuntia* due to similar moisture levels. If different plants are similar in leaf moisture content, it is possible that when creating vegetation indices, the moisture levels indicated in the near-infrared band for the different plants could overlap. This could make it difficult for classification software and algorithms to differentiate between species.

Scientists in Australia have utilized both satellite imagery and UAVs to map and detect invasive species. Ahsan *et al*. (2016) collected data from six weed species in four different areas in Australia to determine if UAV and satellite imagery can be used for weed management programs while eliminating "guess-work" (Ahsan, *et al.*, 2016). First, ground-truthed data were collected to train both multi-scale and multi-class algorithms

and specialized classification algorithms to detect six different weed species: *Nassella trichotoma* (serrated tussock), *Lycium* ferocissium (African boxthorn), *Mimosa pudica* (mimosa), *Sclerolaena birchii* (galvanized burr), *Harrisia martini* (harrisia cactus), and *Pilosella aurantiaca* (orange hawkweed). Human experts trained the algorithms by annotating example weed locations in the imagery collected. Then, both multi-rotor and fixed-wing UAVs were used to collect data. The multi-rotor UAV provided more useful data. These data were then run through the algorithms. The authors achieved detection accuracy of 73% (serrated tussock), 80% (African boxthorn), 73% (mimosa), and 89% (galvanized burr). The automated detection of weeds greatly reduces the manual effort needed to conduct weed surveys, thereby increasing spatial and temporal scope of surveys. The results from this study provide a promising foundation for the use of UAVs in invasive plant detection.

After performing extensive background research, we hypothesized that unique spectral signatures could be created to identify *Opuntia* using information from vegetation indices created using images collected from a multispectral sensor. We also hypothesized that spectral signatures can be developed to differentiate between different species of succulent plants and that UAV-based analysis will produce results that strongly correlate with *in situ* location efforts. The goal of this project is to minimize the environmental dangers and costs of finding and battling invasive species.

METHODS

Study Area

Prickly pear, consumed by humans and other animals, are very cold-tolerant cacti and proliferate the most in the summer, thriving in areas with long summers and mild winters (CABI, 2020). Like other cacti, prickly pear grows exceptionally well in arid and semi-arid climates (Arba *et al.*, 2017). The study areas on and around Balule Nature Reserve have the ideal climate for prickly pear and other succulents to proliferate.

Balule Nature Reserve is a private nature reserve that is a part of the Associated Private Nature Reserves (APNR) of Kruger Park. Located in the Limpopo province of South Africa, Balule borders western Kruger National Park and is characterized as part of the lowveld savanna with a semi-arid climate (Olifants West Nature Reserve, 2015). In recent decades, the area has received an annual average rainfall of 415 mm, categorizing it as semi-arid savannah (Wade, 2016). Balule is known to have stable and moderate levels of perennial grasses, but vegetation levels and conditions are highly dependent on annual rainfalls and climate changes (Peel, 2015). The last decade has seen lower amounts of annual rainfall and more frequent droughts, causing a decrease in the amount of forage during the dry season. This area of Limpopo experiences mild winters and very hot summers with variable rainfall and wildfires. Some common plants and woody trees in Kruger National Park and present in the study areas are red bush willow (*Combretum apiculatum*), knobthorn (*Acacia nigrescens*), grasses of the genus *Eragrostis* (Scholtz *et al.*, 2014), and velvet raison (*Grewia flava*) (Peel, 2015). These plants were seen

commonly among the study areas and were present around the prickly pear plants located for study.

Plots of land in Balule and the surrounding area were designated as flight plots based on criteria such as level of accessibility and vegetation and prickly pear distribution. The plots were either known to have prickly pear, contained no prickly pear, or had unknown levels of prickly pear, if any. We chose 20 sites ranging from 0.9 to 3.9 ha. A map of the reserve was used to select roughly rectangular plots in these areas, and the GPS coordinates of the plots were obtained using ArcGIS. With assistance from reserve personnel and volunteers, we surveyed these plots on foot for prickly pear from May 24th, 2018 to June 19th, 2018. The GPS coordinates of any prickly pear found were recorded. A comprehensive list of the coordinates of the four corners and the locations of the prickly pears in the plots is in **Table 1**.

To ensure that the data could be georeferenced, each of the four corners were marked with large white rocks that were visible in the images captured. The same was done with each known prickly pear; a rock spray-painted white or white plastic bag was placed two meters away from the plant in the direction of the sun and the GPS coordinates were recorded again for accuracy. In order to minimize the effects of shadows when analyzing the data, a time frame was chosen in which the sun was at its highest point, reducing the prominence of shadows in the images captured. For this reason, all flights were completed between 11:00 a.m. and 1:00 p.m. local time. The above process was repeated for one plot containing *Cereus jamacaru* (Queen of the Night), one plot containing *Aloe vera*, and two plots containing *Euphorbia ingens* (euphorbia).

If different plants are similar in leaf moisture content, it is possible that when creating vegetation indices, the moisture levels indicated in the near-infrared band for the different plants could overlap. This could make it difficult for classification software and algorithms to differentiate between species. Some plants we considered for possible confusion were Aloe Vera, plants of the genus *Euphorbia*, and Queen of the Night, a flowering cactus also considered an invasive species in South Africa. However, use of other spectral bands or visual assessment of composite images may allow us to distinguish species.

Hardware, Software, and Data Acquisition

Sensor- The Parrot Sequoia™ agricultural sensor has two main components that ensure accurate and reliable data acquisition (Parrot, 2019). The first is the Multispectral Sensor, which contains four, 1.2-megapixel monochrome sensors: green (550 nm - 40 nm), red (660 nm - 40 nm), red edge (735 nm - 10 nm), and near infrared (790 nm - 40nm). The multispectral sensor also has one, 16-megapixel RGB sensor. The second component, the Sunshine sensor, has a GPS module, an SD card slot, 2 GB internal storage, and is also used to minimize the effects of variations in light during image capture.

Setup- The DJI Phantom Pro 3™ (DJI, 2020) originally came with a camera and gimble for aerial visual imagery. This apparatus was detached from the UAV and the Parrot Sequoia sensor was connected to the main power source. A 32 GB SD card was inserted into the Sunshine Sensor, which we mounted above the body of the UAV. Once the appropriate parts were assembled, the UAV controller was wirelessly connected to the drone through the PrecisionFlight™ (PrecisionHawk, 2010) application accessible on

an iPhone 8. In order to ensure a precise flight that could be monitored at all times, Precisionflight, which is a flight planner app, was used to map and control each flight.

Using the information collected from surveying each plot and marking the appropriate locations, I used the GPS coordinates of each corner to create a map of the plot. On the interface of the app, the flight path that the UAV was predicted to take could be manipulated; the overall flight distance and time changed based on what path was chosen. The above-surface altitude at which the UAV flew was set at 40 meters for every flight. Only one battery could be used at a time in the UAV, so battery life was a major factor when determining flight paths and plot areas. The sensor provided its own WiFi network that allowed the user to access the Parrot Sequoia user interface, view the sensor's specifications, and manipulate the sensor's settings. The user interface enabled the controller to change parameters such as whether the images should be stored onto the SD card or internal storage and at what distance interval each image should be taken when set to capture images based on GPS location. For all flights, the sensor was set to capture an image every five meters, including take-off and landing. Image overlap is an important feature when collecting aerial images.

When a mapping software is "stitching" the images together, increased overlap between images helps in creating a better three-dimensional scene or seamless two-dimensional one (Drones Made Easy, 2020). Based on altitude and flying speed, we determined that a five-meter overlap was adequate. Before each flight, the sensor had to be activated through the interface so that the images would automatically be captured once flight began. The "Come Home" function of the UAV allowed the drone to automatically land from where it took off by recording the GPS coordinates of this

location. This function is automatically utilized if the battery runs low during flight and for un-piloted flights. However, the drone would often land a few meters away from where it took off. Because of the dense vegetation and obstructions around takeoff locations, manual control of landing was often required using the controller, which had full access to manipulate the drone's actions during flight. Once each flight was complete, the acquired images were transferred to a hard drive, along with a document containing the GPS coordinates of each corner and prickly pear plant coordinates paired with pictures of each plant taken on an iPhone.

Data Analysis- Prickly Pear

A mapping software was chosen that had the features necessary to accomplish our basic goals. Pix4Dmapper (Pix4D, 2020) is a cloud-based software that allows the user to import images taken on the Parrot Sequoia. These images can then be processed in a multitude of ways that highlight various aspects of the plot flown. The initial processing stage allows for the input of ground control points (GCPS), calibration of various camera parameters, and geolocation of GPS coordinates and GCPs. The second processing step builds on the data created in the first step to create a point cloud and 3D textured mesh that represent and visualize the shape of the model presented in the map. The third and final processing step produces a digital surface model, a 2D orthomosaic map, a reflectance map, and an index map. The index map is created by utilizing information extracted from each pixel to determine the bandwidth values at each pixel's location. The reflectance values from each bandwidth (red, green, blue, red edge, and near infrared) are then combined and processed through an algorithm, which is specific to the index being produced.

The software also allows the user to use predefined vegetation indices or input algorithms for their own preferred index. Pix4dDapper has a pre-programmed NDVI (Normalized Difference Vegetation Index) algorithm, so for every map produced, an NDVI map was created. The equation used to produce NDVIs is $\boldsymbol{NDVI} = \frac{(\boldsymbol{NIR}-\boldsymbol{Red})}{(\boldsymbol{NIR}+\boldsymbol{Red})}$

The data produced in these maps were then exported in the form of geoTIFF and TIF files containing the geographic coordinates for each pixel and its spectral value derived from the NDVI equation. Along with this processing, individual reflectance maps for the green, near infrared, red, and red edge bandwidths were also created. After researching other vegetation indices that would facilitate differentiation based on moisture levels, maps were created using the Optimized Soil Adjusted Vegetation Index (OSAVI) (Rondeaux *et al.*, 1996). The formula used to create maps using the OSAVI is $\boldsymbol{OSAVI} = \frac{(\boldsymbol{NIR}-\boldsymbol{Red})}{(\boldsymbol{NIR}+\boldsymbol{Red}+\mathbf{0.16})}$

Through QGIS™ software, supervised classifications are to be performed by associates at Balule Nature Reserve. In the supervised classifications, the program will be told which pixels included prickly pear. These will be determined through cross referencing the coordinates compiled during field work. By analyzing the spectral values at these pixels, the computer will assign prickly pear with a specific spectral signature. This signature will then be used to analyze imagery from plots with unknown amounts of prickly pear and identify pixels that potentially have prickly pear.

RESULTS

Table 1 shows each site flown and the date at which it was completed and includes the coordinates of the four corners of each plot.

Site Date and Number	4 Corner Coordinates
5-24-18 site 1	(-24.19657, 30.81456), (-24.19620, 30.81507), (-24. 19696, 30.81501), (-24.19726, 30.81506)
5-24-18 site 2	(-24.19629, 30.8155), (-24.19639, 30.815544), (-24.19667, 30.81552), (-24.19671, 30.81576)
5-24-18 site 3	(-24.19338, 30.81689), (-24.19370, 30.81685), (-24.19326, 30.81754), (-24.19353, 30.81748)
5-25-18 site 1	(-24.21402, 30.88278), (24.21365, 30.88323), (-24.21351, 30.88336), (-24.21357, 30.88222)
5-25-18 site 2	(-24.21726, 30.88766), (-24.21657, 30.88830), (-24.21767, 30.88889), (-24.21776, 30.88825)
5-25-18 site 3	(-24.21726, 30.88766), (-24.21657, 30.88830), (-24.21767, 30.88889), (-24.21776, 30.88825)
5-28-18 site 1	(-24.18631, 30.84628), (-24.18623, 30.84755), (-24.18803, 30.84758), (-24.18856, 30.84909)
5-28-18 site 2	(-24.18695, 30.84102), (-24.18695, 30.84267), (-24.18905, 30.84164), (-24.18899, 30.84279)
5-29-18 site 1	(-24.18860, 30.82835), (-24.18863, 30.82980), (-24.19034, 30.83030), (-24.19035, 30.82853)
5-29-18 site 2	(-24.18812, 30.83166), (-24.18812, 30.83315), (-24.18998, 30.83324), (-24.19003, 30.83178)
5-30-18 site 1	(-24.22504, 30.95387), (-24.22411, 30.95457), (-24.20539, 30.85571), (-24.20551, 30.85477)
5-31-18 site 1	(-24.19519, 30.91610), (-24.19547, 30.91710), (-24.19465, 30.91730), (-24.19428, 30.91548)
5-31-18 site 2	(-24.20439, 30.85533), (-24.20451, 30.85431), (-24.20539, 30.85571), (-24.20551, 30.85477)
6-1-18 site 1	(-24.19562, 30.82954), (-24.19380, 30.82885), (-24.19409, 30.82961), (-24.19542, 30.83046)
6-1-18 site 2	(-24.19756, 30.82978), (-24.19782, 30.83131), (-24.19521, 30.83166), (-24.19567, 30.82994)
6-1-18 site 3	(-24.19590, 30.82915), (-24.19732, 30.82910), (-24.19710, 30.82861), (-24.19542, 30.82833)
6-15-18 site 1	(-24.19195, 30.86355), (-24.19206, 30.86672),

	(-24.19296, 30.86646), (-24.19301, 30.86414)
6-16-18 site 1	(-24.19112, 30.86183), (-24.19102, 30.86308), (-24.19325, 30.86330), (-24.19326, 30.86218)
6-16-18 site 2	(-24.18015, 30.86319), (-24.18054, 30.86289), (-24.18068, 30.86339), (-24.18043, 30.86398)
6-19-18 site 1	(-24.22018, 30.86956), (-24.22012, 30.86646), (-24.22105, 30.86961), (-24.22100, 30.86650)

Table 1: Flight dates, site number, and corner coordinates.

Figure 2 shows the orthomosaic map created of a plot after the initial processing stage is completed. This shows the entire plot flown with the normal RGB camera images. **Figure 3** shows the same map from 5-24 site 2 after an NDVI has been created using the data acquired.

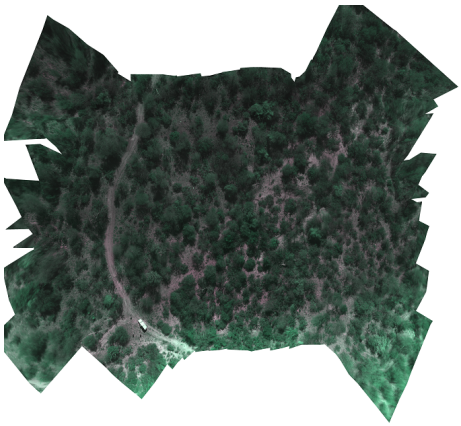

Figure 2: Orthomosiac map of 5-24 site 2

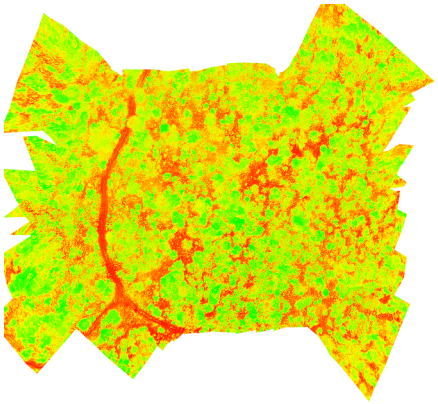

Figure 3: NDVI map of 5-24 site 2

The following figures (**Figures 4-12**) display the maps for Site 1, collected on June 15, in RGB, green, near infrared, red, red-edge, NDVI, and OSAVI.

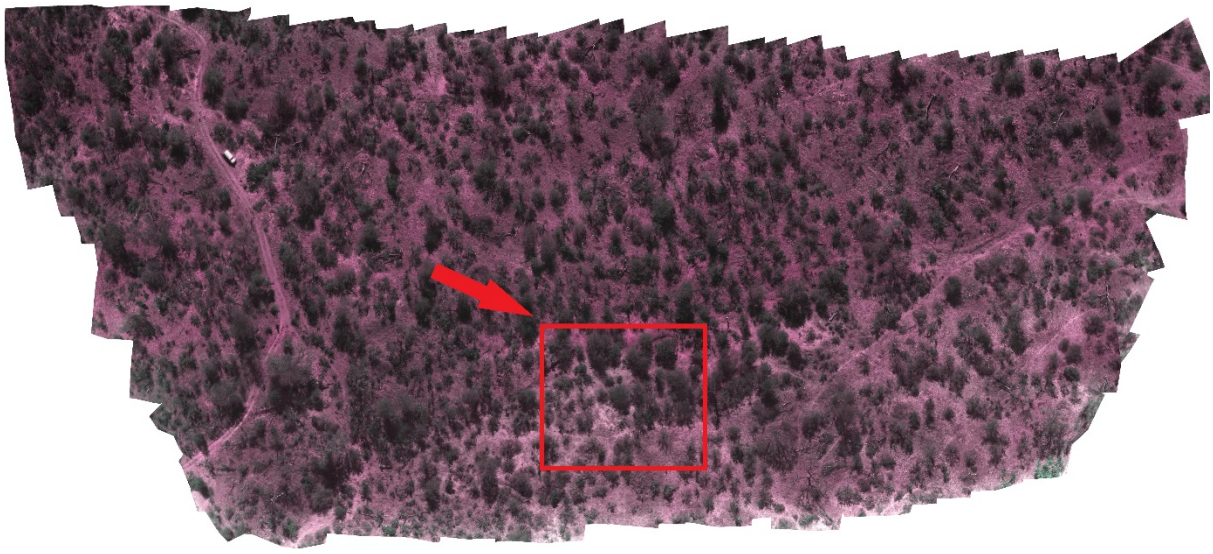

Figure 4: Orthomosaic map of 6-15 site 1, area with prickly pear enclosed in red square

Figure 5: Picture of prickly pear from 6-15 site 1

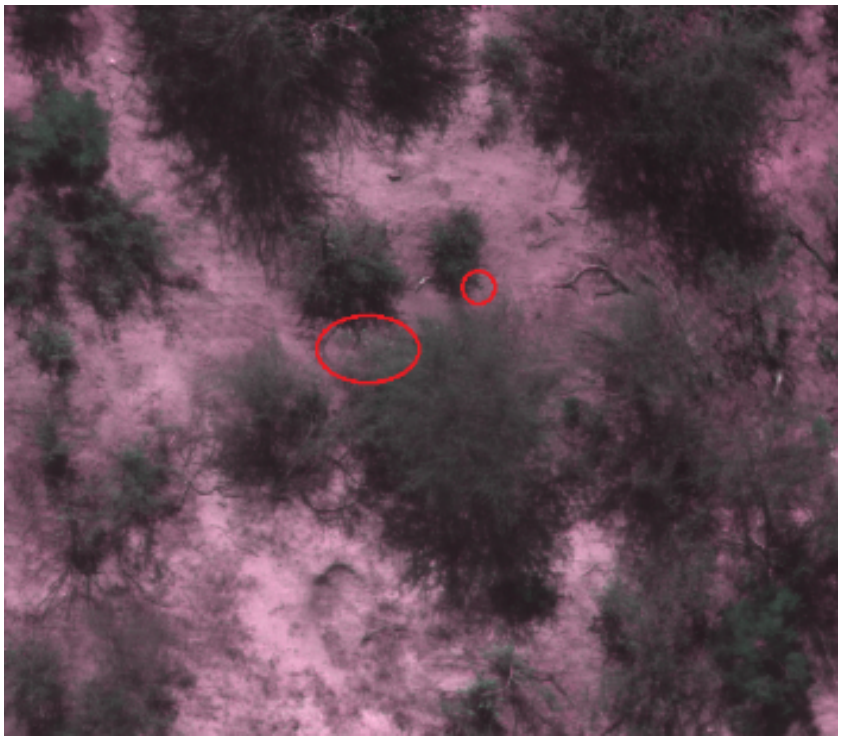

Figure 6: Aerial view of the orthomosaic map from 6-15 site 1 with prickly pear locations circled in red

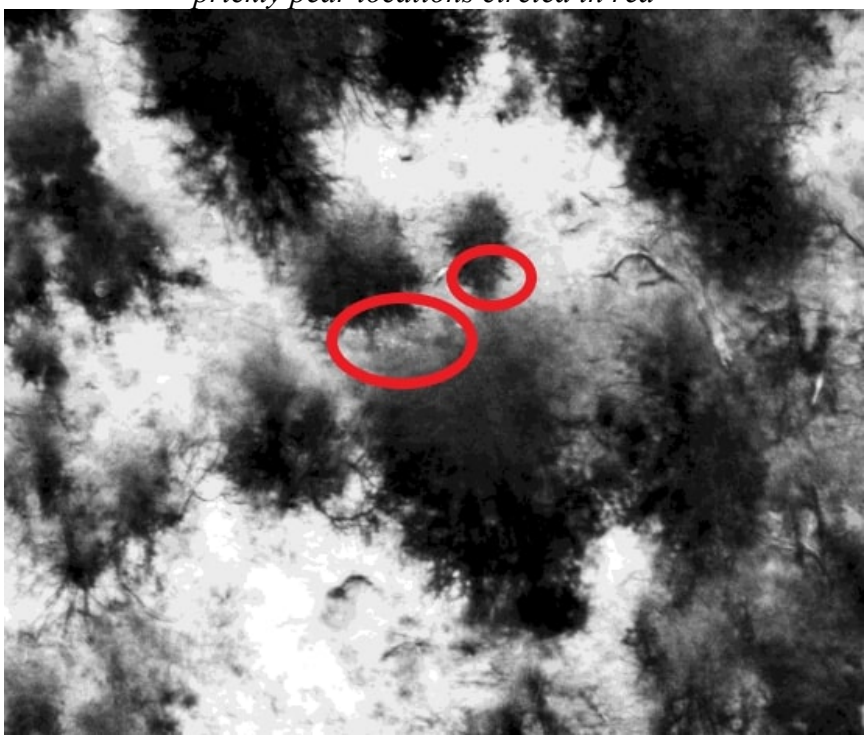

Figure 7: Aerial view of the green reflectance map from 6-15 site 1 with prickly pear locations circled in red

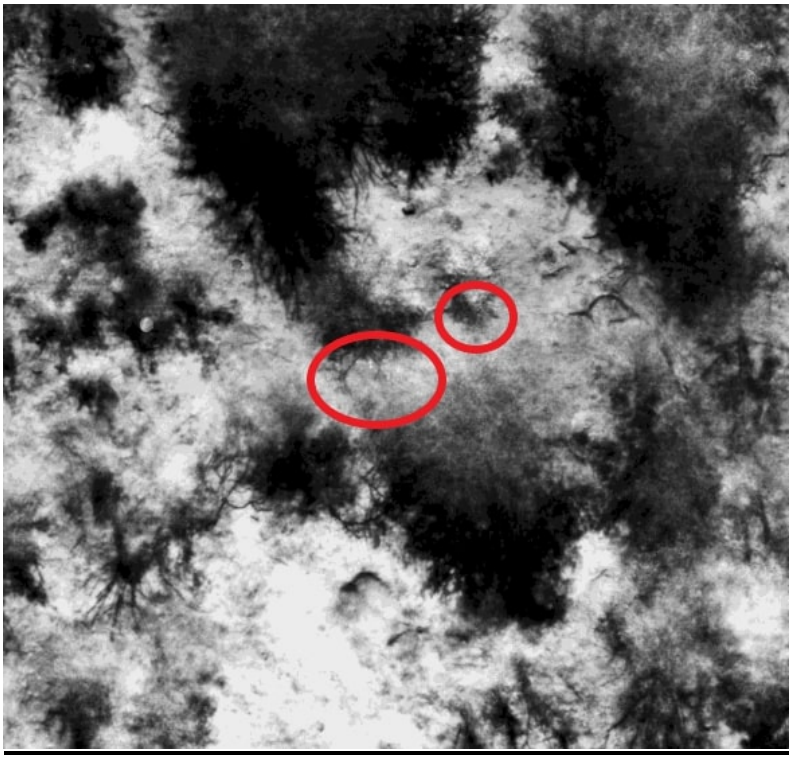

Figure 8: Aerial view of the near infrared reflectance map from 6-15 site 1 with prickly pear locations circled in red

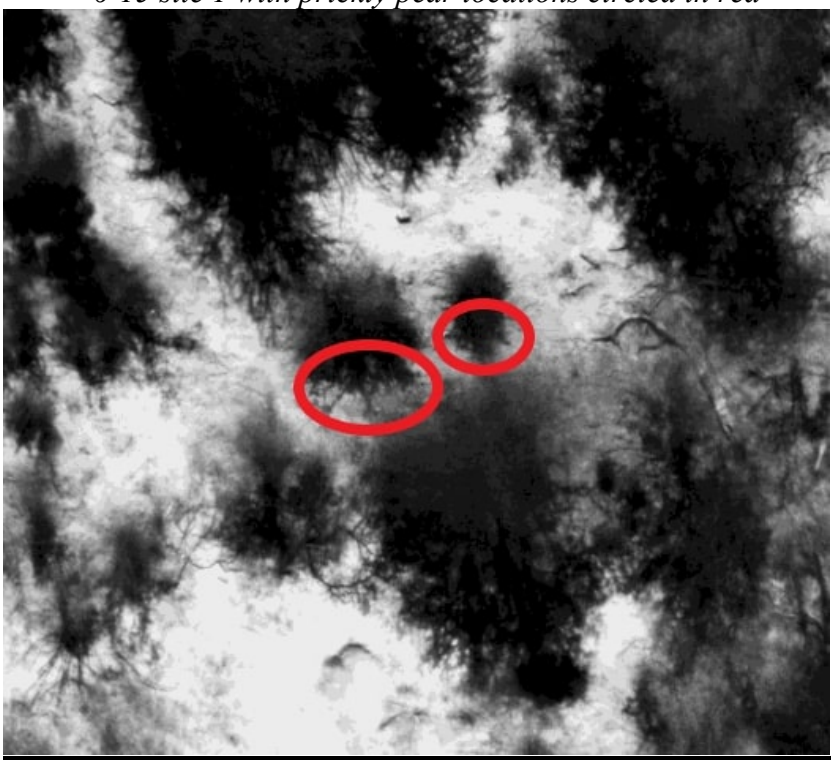

Figure 9: Aerial view of the red reflectance map from 6-15 site 1 with prickly pear locations circled in red

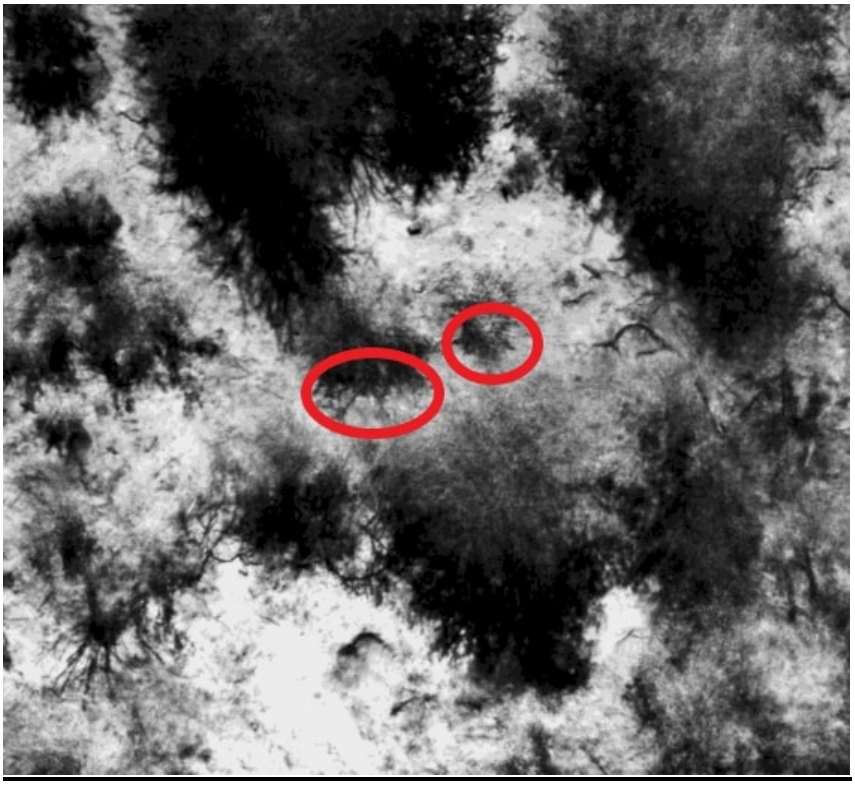

Figure 10: Aerial view of the red edge reflectance map from 6-15 site 1 with prickly pear locations circled in red

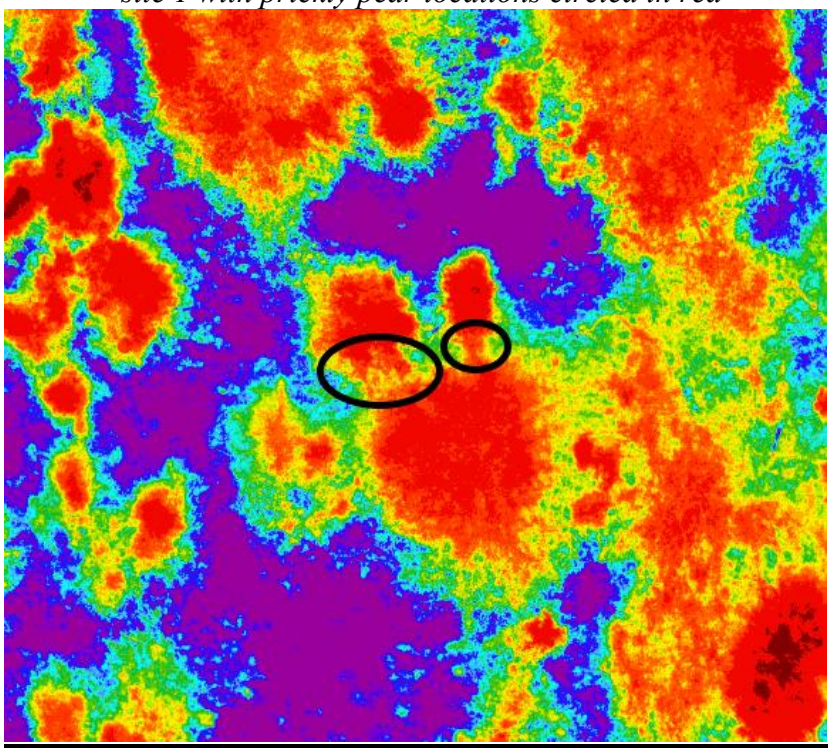

Figure 11: Aerial view of the NDVI map from 6-15 site 1 with prickly pear locations circled in black

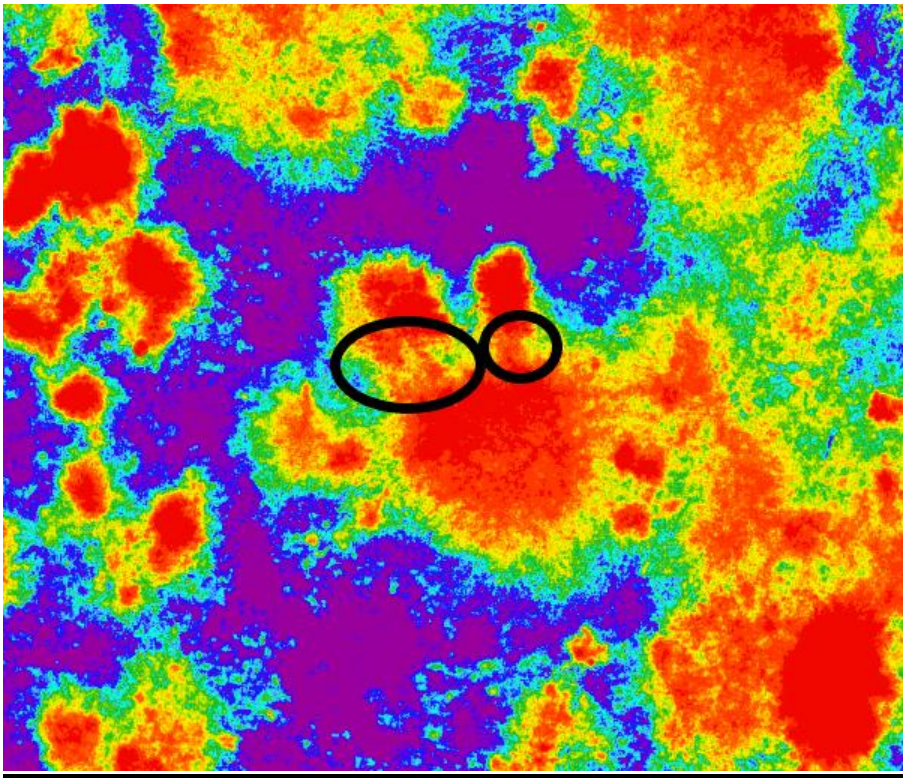

Figure 12: Aerial view of the OSAVI map from 6-15 site 1 with prickly pear locations circled in black

After creating maps of both the indices and all of the reflectances in Pix4Dmapper, I chose a site which contained a considerable prickly pear collection and used the software TNTatlas™ (TNTatlas, 2020) to locate the plants using GPS coordinates. After precisely determining where two of the many prickly pear plants was for this site, I circled the area in each of the seven maps. Although this site had many prickly pear locations, I chose the most heavily inhabited area, opting to forgo locating the very small or individual plants as these would be very difficult to see from the altitude at which the images were taken. After studying these images, I concluded that both the green and near infrared reflectances best highlighted prickly pear. While the brightness of the circled area varies between reflectances and indices, it is hard to distinguish our preferred vegetation due to lack of classifications.

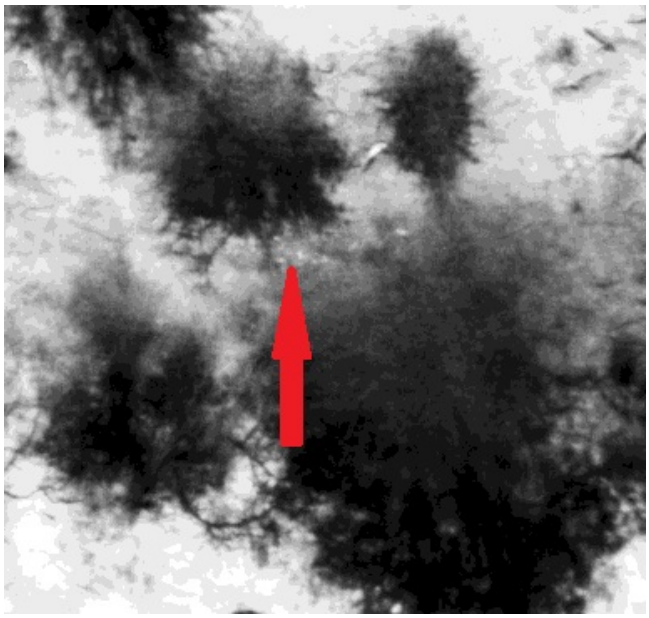

Figure 13: Zoomed in view of green reflectance map distinguishing prickly pear

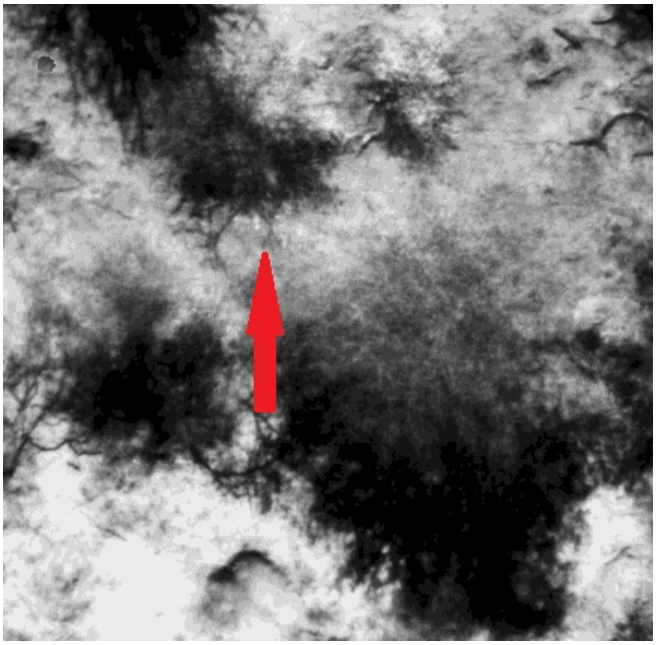

Figure 14: Zoomed in view of near infrared reflectance map distinguishing prickly pear

.

DISCUSSION

The two vegetation indices we used were NDVI and OSAVI. NDVI assists in differentiating between plants and soil through NIR and red reflectance values (MicaSense, 2020). NDVIs are most effective when using data collected in areas with little to medium canopy density. We collected our data in May and June of 2018, during the winter season when vegetation and green cover were relatively low due to low rainfall and inadequate temperatures. This, in theory, facilitated a higher NDVI sensitivity. The NDVI, while one of the leading indices for measuring vegetative properties using remote sensing applications, can often be less reliable and more vulnerable to solar geometry, soil background, and atmospheric effects than other indices more tailored to aerial data acquisition (Rondeaux *et al*., 1996). Soil adjusted vegetation indices perform better at measuring specific vegetation properties than NDVIs when the soil background is unknown, specifically the optimized soil adjusted vegetation index (OSAVI) (Rondeaux *et al.*, 1996). In the OSAVI algorithm, 0.16 serves as the soil adjustment coefficient (MicaSense, 2020). This coefficient effectively reduces NDVI's soil background reflectance and variable environment condition sensitivity. While computer classifications are part of the future direction of this product, it is hard to tell from simple visual analysis what the different various vegetation indices tell us about the spectral signatures of prickly pears.

While careful considerations of study area, technological restrictions, and data analysis were taken before, during, and after field data acquisition, there are some areas

in which improvement could be made. Firstly, we ran into many technical issues throughout the process. This could have been avoided by fully preparing the equipment before beginning field work. However, the sensor could not have been attached to the drone beforehand due to travel restrictions and safety measures. A period of time directly before beginning data acquisition at Balule was spent figuring out the software, firmware, and user interfaces of the many phone applications used to test and fly the drone. It would have been ideal to become familiar with the equipment before travelling to South Africa. Towards the end of field work, the sensor malfunctioned, cutting short the amount of data we wanted to collect. By studying the UAV and software used beforehand, this issue likely could have been fixed while still performing field work.

Our partners in South Africa are currently working to perform supervised and unsupervised classifications on all of the flights performed. They are working with GIS software to assign prickly pear a unique signature and to attempt to identify prickly pear in the plots we flew with minimal false positive results. The information gathered in this study is intended to make easier the process of invasive species control. We hope that once our result goals are reached, we can create a pathway for scientists and conservation biologists to battle harmful species in a safe and manageable way, minimizing injury and time and financial costs.

REFERENCES

Ahsan, N., Xu, Z., Murphy, R., & Sukkarieh, S. (2016). The practical application of state-of-the-art un-manned aerial vehicles and imaging technology to on farm management of invasive weeds. *Australian Centre for Field Robotics.*

Anderson, D. R., Laake, J. L., Crain, B. R., Burnham, K. P. (1979). Guidelines for line transect sampling of biological populations. *The Journal of Wildlife Management*. 43(1), 70-78. https://dx.doi.org/10.2307/3800636

Arba, M., Falisse, A., Choukr-Allah, R., Sindic, M. (2017). Biology, flowering and fruiting of the cactus *Opuntia* spp.: a review and some observations on three varieties in Morocco. *Brazilian Archives of Biology and Technology*. 60. 1-11. http://dx.doi.org/10.1590/1678-4324-2017160568

Buckland, S. T. (1985). Perpendicular distance models for line transect sampling. *Biometrics*. 41(1), 177-195. https://dx.doi.org/10.2307/2530653

Centre for Agriculture and Bioscience International [CABI] (n.d.). *Opuntia ficus-indica* (prickly pear). *Invasive species compendium.* https://www.cabi.org/isc/datasheet/37714

Centre for Agriculture and Bioscience International [CABI] (2019). Biological control of invasive plants. https://www.cabi.org/what-we-do/cabi-centres/biological-control-of-invasive-plants/

Candiago, S., Remondino, F., De Giglio, M., Dubbini, M., & Gattelli, M., (2015). Evaluating multispectral images and vegetation indices for precision farm applications from UAV images. *Remote Sensing.* 7(4), 4026-4047. https://dx.doi.org/10.3390/rs70404026

Carl, C., Landgraf, D., van der Maaten-Theunissen., M., Biber, P., & Pretzsch, H., (2017). *Robinia pseudoacacia* L. flower analyzed by using an unmanned aerial vehicle (UAV). *Remote Sensing*. *9*(11), 1091; https://doi.org/10.3390/rs9111091

DJI (n.d.). Phantom Series. https://store.dji.com/shop/phantom-series?from=menu_icon

Drones Made Easy (2020). Overlap management. https://support.dronesmadeeasy.com/hc/en-us/articles/207743803-Overlap-Management

Hall, R. A., Papierok, B., (1982). Fungi as biological control agents of arthropods of agricultural and medical importance. *Parisitology.* 84 (4), 205-240. https://doi.org/10/1017/S0031182000053658

Hegazy, I. R. & Kaloop, M. R., (2015). Monitoring urban growth and land use change in detecting with GIS and remote sensing techniques in Daqahlia governorate Egypt. *International Journal of Sustainable Built Environment*. 4(1), 117-124. https://doi.org/10.1016/j.ijsbe.2015.02.005

Invasive Species South Africa, (2019). Retrieved from http://www.invasives.org.za/resources/marketing-materials#regional-iap-booklets-a4

Joshi, C., de Leeuw, J., & Van Duren, I. C., (2004). Remote sensing and GIS applications for mapping and spatial modeling of invasive species. *ISPRS*. 35, 669-677.
.

Joshi, N., Baumann, M., Ehammer, A., Fensholt, F., Grogan, K., Hostert, P., Jepsen, M. R., Kuemmerle, T., Meyfroidt, P., Mitchard, E. T. A., Reiche, J., Ryan, C. M., & Waske, B., (2016). A review of the application of optical and radar remote sensing data fusion to land use mapping and monitoring. *Remote Sensing*. *8*(1), 70. https://doi.org/10.3390/rs8010070

Lemke, D., Schweitzer, C. J., Tadesse, W., Wang, Y., Brown, J.A. (2013). Geospatial assessment of invasive plants on reclaimed mines in Alabama. *Invasive Plant Science and Management*. 6(3), 401-410.

Matese, A., Toscanp, P., Di Gennaro, S. F., Genesio, L., Vaccari, F. P., Primicerio, J., Belli, C., Zaldei, A., Bioanconi, R., & Gioli, B., (2015). Intercomparison of UAV, aircraft and satellite remote sensing platforms for precision agriculture. *Remote Sensing*. *7*(3), 2971-2990. https://doi.org/10.3390/rs70302971

MicaSense (n.d.). An overview of the available layers and indices in Atlas. https://support.micasense.com/hc/en-us/articles/227837307-An-overview-of-the-available-layers-and-indices-in-Atlas

MicroImages (2020). TNTatlas 2018. MicroImages, Inc. https://www.microimages.com/downloads/tntatlas.htm

Olifants West Nature Reserve (2015). Wardens Report.

Parrot (2019). Parrot Sequoia +. Parrot Drones SAS. https://www.parrot.com/business-solutions-us/parrot-professional/parrot-sequoia

Peel, M. (2015). Ecological monitoring: Association of Private Nature Reserves (Timbavati, Umbabt, Klaserie, and Balule) (Report No. 13-2015).

http://umbabat.com/wp-content/uploads/2019/04/APNR-Ecological-Report-2015.pdf

Pix4D (2020). Pix4D Mapper. Pix4D SA. https://www.pix4d.com/product/pix4dmapper-photogrammetry-software

PrecisionHawk (2010). Precisionflight free. https://www.precisionhawk.com/precisionflight

Richardson, D. M. & Van Wilgen, B. W., (2004). Invasive alien plants in South Africa: how well do we understand the ecological impacts? *South African Journal of Science.* 100(1), 45-52.

Rignanese, L. (2005). Indian fig 2 – *Opuntia ficus-indica*. [Photograph]. Wikipedia. https://en.wikipedia.org/wiki/File:Indian_Fig_2_-_Opuntia_ficus-indica.jpg

Rondeaux, G., Steven, M., Baret, F., (1996). Optimization of soil-adjusted vegetation indices. *Remote Sensing of the Environment, 55*(2), 95-107. https://doi.org/10.1016/0034-4257(95)00186-7

Scholtz, R., Kiker, G. A., Smit, I. P. J., Venter, F. J., (2014). Identifying drivers that influence the spatial distribution of woody vegetation in Kruger National Park, South Africa. *Ecosphere*. 5(6), 1-12. https://doi.org/10.1890/ES14-00034.1

Turner, W., Spector, S., Gardiner, N., Fadeland, M., Sterling, E., & Steininger, M., (2003). Remote sensing for biodiversity science and conservation. *TRENDS in Ecology and Evolution.* 18(6), 306-314. https://doi.org/10.1016/S0169-5347(03)00070-3

USFWS (2012. The cost of invasive species. https://www.fws.gov/verobeach/PythonPDF/CostofInvasivesFactSheet.pdf

Wade, S., (2016). The effects of drought on diets of apex predators in the South African lowveld inferred by fecal hair analysis. *Honors College Capstone Experience/Thesis Projects*. Paper 669. http://digitalcommons.wku.edu/stu_hon_theses/669

Zengeya, T., Ivey, P., Woodford, D. J., Weyl, O., Novoa, A., Shackleton, R., Richardson, D., & van Wilgen, B., (2017). Managing conflict-generating invasive species in South Africa: Challenges and trade-offs. *Bothalia - African Biodiversity & Conservation.* 47(2), 1-11. https://dx.doi.org/10.4102/abc.v47i2.2160

Zhang, C. & Kovacs, J.M., (2012). The application of small unmanned aerial systems for precision agriculture: A review. *Precision Agriculture*. 13(6), 693-712. https://doi.org/10.1007/s11119-012-9274-5